TIME-RESOLVED REFLECTIVITY STUDY OF PULSED-LASER-IRRADIATED, Si_3N_4-CAPPED GaAs

by

AJIT BHAT

B.tech, I.I.T.-Kanpur, 1982, M.tech, I.I.T.-Delhi, 1984

A MASTERS'S THESIS

submitted in partial fulfillment of the

requirements for the degree

MASTER OF SCIENCE

Department of Physics

KANSAS STATE UNIVERSITY

Manhattan, Kansas

1987

Approved by:

TABLE OF CONTENTS

Page

LIST OF FIGURES

LIST OF TABLES

ACKNOWLEDGEMENTS

CHAPTER

1. Introduction 1

2. The Experimental Set-up 6

   A Transient Reflectivity Measurements 6

   B Ellipsometric Measurement of Cap thickness : Null Ellipsometry 22

3. Analysis of Data : Determination of temperature-dependent refractive indices of GaAs and Si_3N_4..... 27

   A Features of Time-resolved Reflectivity Traces .. 32

   B Multiple Beam Interference 38

   C Determination of refractive indices of GaAs and Si_3N_4 44

4. Conclusion 54

APPENDIX

   A Fresnel coefficients for p- and s-polarizations..57

   B Listing of program for computing Reflectivity as a function of Cap thickness for p- and s-polarization 58

   C Listing of program used to operate the digitizer 62

REFERENCES 65

ABSTRACT 68

LIST OF FIGURES

Figure		Page
1	Experimental set-up for time-resolved reflectivity measurement	8
2	Annealing without beam homogenizer: photograph of annealed spot	11
3	Arrangement to do homogeneous annealing	14
4	Pulse shapes of excimer and dye laser outputs	17
5	The 7912 AD Digitizer scan converter target	21
6	Ellipsometric Measurement of Cap thickness	23
7	Effect of dopants on absorption coefficient of GaAs	31
8	Features of Reflectivity vs Time trace for capless samples during pulsed laser irradiation	34
9	Reflectivity vs Time for capped samples	37
10	Multiple Beam Interference: thin transparent layer on a substrate	41
11	Polarization dependence of Reflectivity	43
12	Reflectivity vs Cap thickness for the probe beam : p- and s-polarization	47
13	Reflectivity traces used to determine refractive indices of GaAs and Si_3N_4	49
14	Reflectivity vs Time traces obtained during dye laser annealing	53

LIST OF TABLES

Table		Page
1	Reflection Ellipsometry: Matching of computed and experimental values to determine cap thickness	29
2	Suggested values of the temperature-dependent refractive indices of GaAs and Si_3N_4	45
3	Calculated and observed ratios for the change in reflectivity of the samples when the GaAs substrate is solid and just below the melting point	50
4	Calculated and observed ratios for the change in reflectivity of the samples when the GaAs substrate is in the molten phase	50

ACKNOWLEDGEMENTS

I would like to thank my major professor Dr. Alvin Compaan for his invaluable guidance and his patience during the course of the work.

I am thankful to Dr. Andrzej Rys and Dr. C. M. Sorensen for serving on my committee.

Amongst the Graduate Students, I appreciate the help of Huade Yao and Mandar Dange from Physics Department, Gi Ho Jeong and Glenn Lo from Chemistry Department, and Arkady Horak and Timothy Chin from Electrical Engg. in preparing for the experiments.

The partial support of Wright Patterson Air Force Base, Dayton Oh, is gratefully acknowledged.

CHAPTER 1

INTRODUCTION

A rapid growth of interest in laser processing of semiconductors can be traced to the mid-seventies when laser irradiation of ion-implanted Si and GaAs was first tried.[1] The purpose was to electrically activate the dopants and remove the lattice damage caused by ion implantation. A considerable body of data now exists on GaAs, which is an important compound semiconductor for device applications. Yet, the information available is not nearly as complete as it is for Si, which is an elemental semiconductor, and the search to find a satisfactory method for the processing of GaAs continues.

The conventional method of high-temperature furnace annealing has the disadvantage that the entire substrate must be heated in order to remove the implantation damage. With laser annealing, however, depending on the wavelength, the radiation is heavily absorbed in a thin surface layer of at most a few hundred nanometers. Thus only the implanted region reaches high enough temperatures to melt and the implantation damage in this region can be repaired while the substrate is left unaffected. A number of authors have noted that good crystallinity is obtained following laser melting and rapid solidification of GaAs and some have used channeling spectra to compare the effectiveness of cw argon-ion laser annealing, furnace annealing, and pulsed-laser

annealing for removal of implantation lattice damage.[2,3] In the channeling spectra obtained from pulsed laser annealed samples, the characteristic peaks of Ga and As have been found to be small and the authors have concluded that liquid phase epitaxial regrowth as obtained with pulsed lasers is far superior to regrowth in the solid phase resulting from other modes of annealing. It is believed that if the annealing energy density is sufficiently high the melt depth penetrates deep into the matrix and all nucleation centers for defects are removed. Another advantage of pulsed-laser annealing is that the equilibrium solubility limits of the implanted ions can be exceeded. RBS and chanelling mesurements have indicated an increase of more than an order of magnitude in solid solubility of certain dopants as compared to those obtained following furnace annealing.[4] A longstanding difficulty with processing of compound semiconductors is surface decomposition. Some of the early studies on thermal annealing indicated As loss during annealing of GaAs. It was also shown that the effect of implantation is to enhance the release of As at temperatures below 500° C by as much as a factor of eight, and to lower the temperature at which significant As release begins from over 600° C to about 200° C.[5,6] It has been suggested that the effect of implantation in enhancing As vaporization can be understood in terms of implantation providing a significant

concentration of vacancies and other defects close to the surface.[6] Initial studies of pulsed annealing of implanted GaAs were motivated, at least in part, by the hope that the short melt duration (~100 ns) during annealing would minimize As loss. However, SEM observations indicated surface decomposition and a Ga-rich surface just as was observed for the other methods of annealing.[7]

Encapsulant layers of Si_3N_4 and SiO_2 have therefore been introduced with the purpose of retaining As during pulsed annealing and thermal annealing of GaAs. TEM studies show that the formation of Ga-rich surface globules can be suppressed with the use of caps.[8,9]. Moreover, improved electrical activation with both n- and P-type dopant ions has also been reported.[9,10,11] A feature of annealing of capped samples is the possible doping of the GaAs substrate by constituents of the capping layer.[10] This can be an advantage if the doped constituent reduces the quenched-in compensating defects in the surface layer that result from rapid solidification. Use of caps, however, is not free of all problems. Our observation (see Fig 9c) that annealing with very high energy densities damages or even "blows away" the cap is consistent with earlier reports. Ripples on the surface of SiO_2 are observed for pulse energy densities above the threshold for melting.[12] These ripples are believed to be formed because of differential stress between the encapsulating layer and molten GaAs.

Although reported results from laser annealing of capped samples indicate improved electrical activity as compared to the results from furnace annealing and laser annealing in the absence of caps, a lack of complete activation of high-dose implants and very little activation of low-dose implants were observed and the electron mobility attained was rather low.[8,13] This has been attributed to the trapping of dopants at antisites or quenched-in compensating defects that result from rapid solidification.[14,15,16] However, these processes are not fully understood and in order to provide a better understanding of the actual mechanism involved, a need exists for more detailed studies of the process.

The experiments that have been performed to understand the phenomenon and to construct theoretical models fall into two broad categories: 1) The conventional post-irradiation measurements such as Rutherford back scattering (RBS), secondary ion mass spectroscopy (SIMS), transmission and scanning electron microscopy (TEM & SEM) and sheet electrical properties measurements & 2) Time resolved measurements during laser irradiation such as optical reflectivity and transmission, electrical conductivity, and temperature-sensitive measurements such as pulsed Raman scattering.

In this thesis, I will discuss time resolved reflectivity measurements that we made using an argon-ion

probe beam while samples of GaAs capped with Si_3N_4 were annealed with $\sim$10 nanosecond excimer laser and dye laser pulses. The reflectivity observed when the GaAs substrate is in the molten phase, or when it has a temperature just below the melting point, can be used to estimate the temperature-dependent refractive indices of GaAs and Si_3N_4. These constants can be useful input parameters for models describing annealing of GaAs.

The lay-out of this thesis is as follows. In Chapter 2, I will discuss the experimental set-up and the equipment used. In Chapter 3, I will discuss the different features of some of the reflectivity traces that were obtained in the course of the experiment. Also included here will be a simple model of multiple-beam interference, which with an appropriate choice for the optical constants, can explain the observed reflectivities. Chapter 4 will have my concluding remarks about the significance of the experiment. The computer programs used while collecting and analyzing the data will be included in Appendices.

CHAPTER 2

THE EXPERIMENTAL SET-UP

The set-up that was used to measure the transient reflectivity of Si_3N_4-capped GaAs samples for a continuous wave probe beam (λ = 514.5 nm) will be discussed here. The probe beam was focussed on to a spot which was irradiated with $\sim$10 ns pulses from an excimer laser (λ = 308 nm) or a dye laser (λ = 728 nm). The change in the reflected beam intensity as a function of time was recorded.

For determining the cap thickness of the two capped samples used, an ellipsometry set-up was required. This too will be described later in this chapter.

Transient Reflectivity Measurement

The Excimer Laser: Fig 1 describes the arrangement that was used for the transient reflectivity measurerments. The excimer laser was Questek Model # 2240-021. The rare gases that can be used to form the operating medium are Ne, Ar, Kr and Xe in certain combinations with HCl or F_2. The laser utilizes the electronic transitions in the rare gas halide molecules to produce intense pulses of ultraviolet light. XeCl was used for the experiment to produce radiation at 308 nm and the standard factory recipe for the gas mixture while using XeCl is as follows.

He (with 5% HCl): 80 mb

Xe: 100 mb

Figure 1 Experimental set-up for time-resolved reflectivity measurement: L=lens L_1, L_2 and L_3 are quartz lenses and are further described in Figure 3, L_4: focal length=24.4 cm, L_5: focal length=4.5 cm, BS=beam splitter, F=filter stand, P=quartz diffusing plate, SM=Sample mount, M=mirror, D=p-i-n photodiode, SF=spike filter

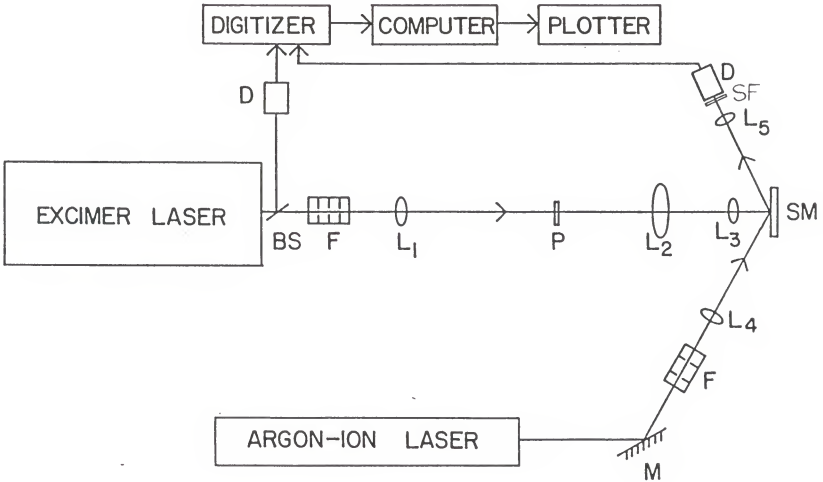
DIGITIZER
COMPUTER
PLOTTER
D
D
SF
L5
EXCIMER LASER
BS
F
L1
P
L2
L3
SM
L4
F
ARGON-ION LASER
M

He: 1100 mb (as buffer gas)

Ne: 3050 mb (as buffer gas)

As much as 150 mJ/pulse is available with a fresh gas mixture and the output energy gradually decreases as the HCl gets depleted because of adsorption on the interior surfaces of the chamber. The gases can be replenished periodically to boost the output. The pulse duration (FWHM) is $\sim$10 ns, the output beam dimensions are 2cm x 1cm and the beam divergence is about 3 mr. The control panel of the laser is equipped with a microprocessor which can be used for several purposes, including changing the composition of gas mixture, and changing the output energy and pulse repetition rate. Annealing energies up to 0.35 J/cm^2 were used and the threshold for damage to the caps was found to be about 0.3 J/cm^2. The pulse energy could be varied either by entering the desired value at the control panel or by inserting filters in the path of the pulses. All energy measurements were made with a laser power meter (Model 3600, Scientech Inc).

Homogeneity of annealed spots

The excimer laser irradiation was first tried by simply focusing the pulses through an astigmatic quartz lens on to the sample to produce spots which were about 1 mm x 1 mm in dimension. The astigmatic lens (with focal lengths of 19.3 cm in the horizontal and 24.5 cm in the vertical plane) was

Figure 2 Annealing without beam homogenizer: photograph of a spot annealed through a 0.5 mm diameter aperture; the variation in the extent of damage to the cap is indicative of beam inhomogenity.

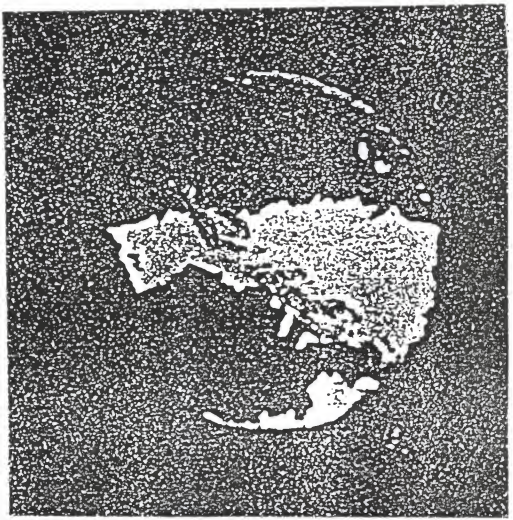
0.5 mm

used because the output from the laser was rectangular in shape, and the lens could be rotated so as to produce spots that were close to square-shaped. However, the annealed spots with this simple arrangement were found to be nonuniform. The variation in the extent of damage to the cap across the annealed spot at an average annealing energy of 0.3 J/cm^2, as seen through a microscope, was an indication of the lack of uniformity (see Fig 2). This lack of uniformity was due to spatial inhomogeneity across the laser pulse, and introducing a quartz diffusing plate in the path of the beam resulted in a more uniform spot. Unlike glass, quartz is transparent to ultra-violet radiation and the diffusing plate was prepared by first uniformly rubbing a circular quartz disk (diam 3/4 ", thickness 1/16 ") with 1 um emery paper and then dipping it in 50% hydrofluoric acid. The laser power available was a limiting factor, and increasing the duration for which the plate was dipped before use gave better transmission but poorer homogeneity. After several trials it was determined that the most satisfactory result is obtained by dipping the plate in hydrofluoric acid for about twenty minutes.

The arrangement that was found most suitable, once again after several trials, was one in which the diffusing plate was placed beyond both of the focal points of the astigmatic lens and the transmitted light collected with a large diameter lens and then focussed on to the sample.

Figure 3 Arrangement to produce homogenuous spots: L_1=quartz astigmatic lens with focal lengths of 19.3 cm and 24.5 cm, P=quartz diffusing plate (diameter=3/4", thickness=1/16"), L_2=quartz collecting lens (diameter=7 cm, focal length=13.5 cm), L_3=quartz focussing lens (diameter=3.8 cm, focal length=10.2 cm).

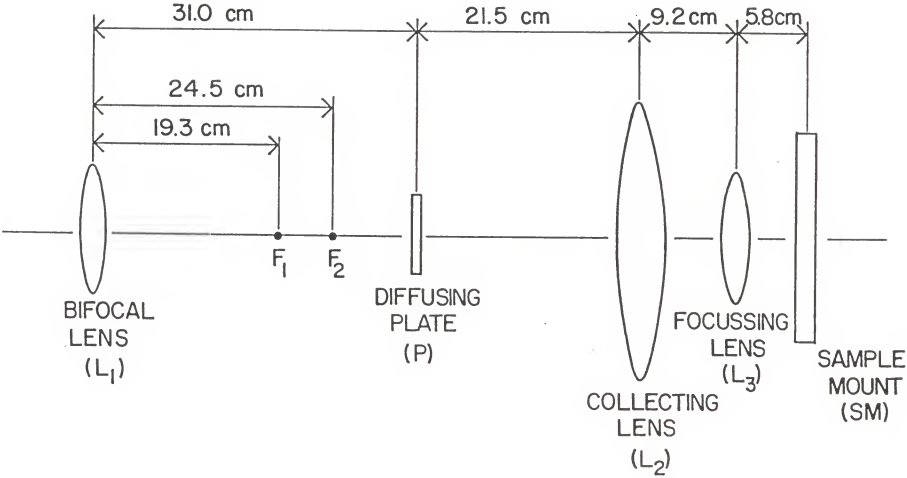
31.0 cm
21.5 cm
9.2cm
5.8cm
24.5 cm
19.3 cm
F1
F2
BIFOCAL LENS (L1)
DIFFUSING PLATE (P)
COLLECTING LENS (L2)
FOCUSSING LENS (L3)
SAMPLE MOUNT (SM)

This arrangement is shown in Fig 3. The position of the collecting lens C and the focussing lens F could be changed to vary the dimensions of the annealed spots and the maximum energy available was dependent on their positions. Thus high energies could be used only for annealing small spots and large spots could be annealed only with low energies. With this arrangement less than 5% of the laser pulse energy was available for annealing, the rest being lost due to reflection at the several surfaces present and due to scattering. Energies up to 0.35 J/cm^2 could be used for annealing spots that were about 1 mm X 1 mm. With the help of ultraviolet sensitive proof paper (Dupont) the variation in intensity was estimated to be less than 10% within this area.

Dye Laser: The experiment was also performed with ~10 ns pulses from a dye laser instead of an excimer laser. In this case, it was not found necessary to use any sort of beam homogenizer. Only a single astigmatic lens (f = 68 cm and 124 cm) was used to focus the pulses on to the sample. The set-up with the excimer laser and the dye laser was otherwise similar. Figure 4 describes the pulse shapes for the two lasers.

The Probe Beam: An argon-ion laser from Laser Ionics, Inc(Model No 551A during excimer laser irradiation and Model No 554A during dye laser irradiation) was used for the probe

Figure 4 Pulse shapes of

(a) Excimer laser output; λ=308 nm.

(b) Dye laser output; λ=728 nm.

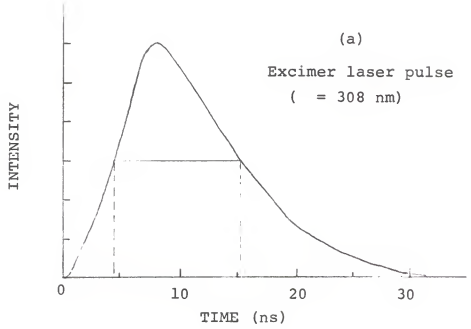
(a)
Excimer laser pulse
(= 308 nm)
INTENSITY
0
10
20
30
TIME (ns)

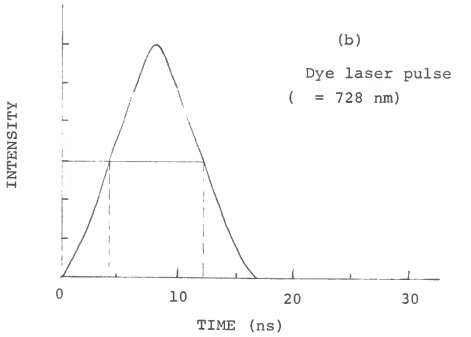
(b)
Dye laser pulse
(= 728 nm)
INTENSITY
0
10
20
30
TIME (ns)

beam. The output from this laser is linearly polarized and the plane of polarization could be rotated with a double Fresnel rhomb polarization rotator. Thus, both p- and s-polarizations (parallel and perpendicular to the plane of incidence, respectively) could be selected for the reflectivity studies. The probe beam was focussed to a spot of about 50 um and made to overlap with the excimer laser spot. The angle of incidence was chosen chosen to be 60° for annealing with the excimer laser and 30° with the dye laser. A HP 5082-4220 silicon p-i-n photodiode (rise time $\sim$1 nanosecond) was used to detect the reflected light. The probe beam power, which could be changed with the use of filters, was chosen so as to ensure that the photodiode was operating in a range in which the output was propotional to the incident intensity.

The GaAs samples were about a millimeter in thickness and 1 cm X 1 cm laterally. They were mounted on a translation stage so as to facilitate x-y movement. Stepper motors and a stepper motor controller (Maxwell Electronics SMC-488A) interfaced to a computer (Zenith PC) were available and were used for providing uniform spacing between consecutive "shots" from the excimer laser. The output from the photodiode measuring the reflected beam intensity was recorded by the digitizer. A portion from the edge of the excimer laser pulse was partially reflected to another photodiode to provide a trigger for the digitizer (see Fig

1). The transient digitizer was found to be very convenient for recording the data and will be described next.

Programmable Digitizer (Tektronix 7912 AD)

The Tektronix 7912 AD programmable digitizer is a wide-bandwidth waveform acquisition instrument with both analog and digital outputs. Two operating modes are provided. In the digital mode, the 7912 AD digitizes either a single-shot or a repetetive waveform and stores it for internal processing or for output on an IEEE 488 bus. Analog outputs are also provided to display the waveform data on a monitor. In the TV mode, the 7912 AD converts a waveform to a composite video output which can be displayed on a TV monitor. The digitizer operates in many ways like an oscilloscope. The input signal is connected to a vertical plug-in to drive the vertical deflection amplifier. A wide range of deflection factors can be selected on the front panel for amplification. The horizontal deflection amplifier can also be driven at different sweep rates.

The major difference between the oscilloscope and the digitizer is that instead of displaying the input waveform as a trace on a phosphorous coated face of a CRT as in the oscilloscope, in the digitizer the input waveform is written on a silicon diode matrix. This array of diodes is formed on an n-type silicon wafer by integrated circuit techniques. In operation, the target substrate is held positive with respect

Figure 5 The scan converter target of the Tektronix 7912 AD Digitizer

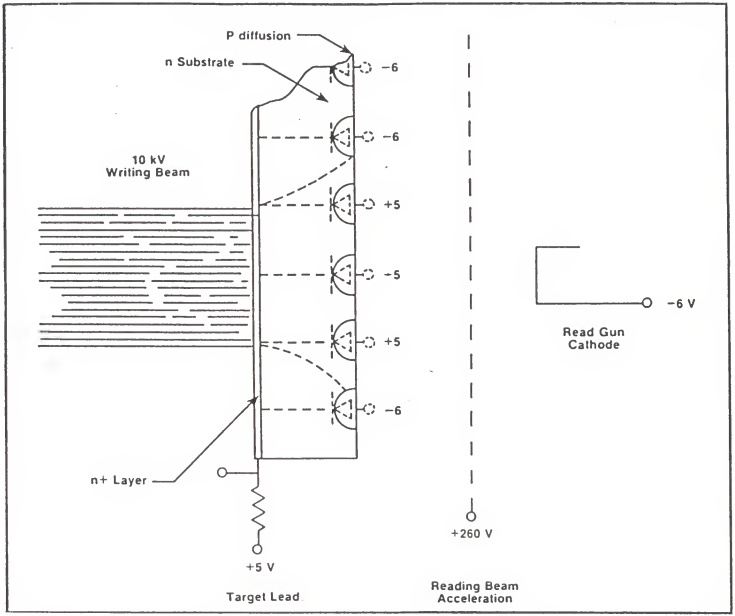
P diffusion
n Substrate
10 kV
Writing Beam
−6
−6
+5
−5
+5
−6
n+ Layer
+5 V
Target Lead
+260 V
Reading Beam
Acceleration
−6 V
Read Gun
Cathode

to the reading gun cathode by the target lead, and is scanned continuously by the reading beam, charging each diode toward the more negative potential diode to reverse-bias it (see Fig 5). The height of the trace of the electron beam from the writing gun varies according to the input signal. Each writing gun electron is accelerated by a 10 KV potential between the gun and the target and creates many electron-hole pairs near the surface. The holes diffuse through the target and drift across the depletion region at the p-n junction, causing the adjacent diodes to conduct and discharge. When the reading beam scans the target, little or no current flows through the target lead at points that were not written and a signal current is detected where the target was written. This output signal is then amplified for further processing. The main feature of the 7912 AD digitizer is high speed performance which gives it a resolution of less than 1 ns and enables it to record rapid changes in the input signal.

Ellipsometric Measurement of Cap Thickness: Null Ellipsometry

The ellipsometric measurement of cap thickness was done with the arrangement suggested by Popov.[17] This has been shown in Fig 6. A beam of parallel light from a He-Ne laser (λ = 633 nm) was first passed through a rotatable polarizer (Glan-Thompson prism) and then through a Soleil Babinet Compensator acting as a $\lambda/4$ plate with fast axis at 45^{o} to the

Figure 6 Ellipsometric measurement of cap thickness: P=Glan-Thompson prism, SBC=Soleil Babinet Compensator used as a quarter wave plate, SM=sample mount, A=polaroid analyzer, S=screen.

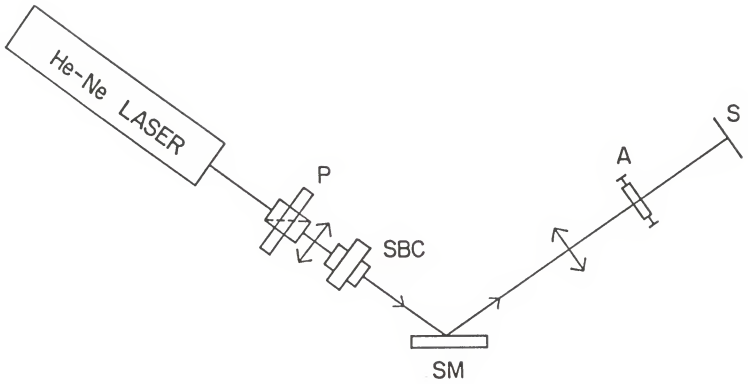
He-Ne LASER
P
SBC
SM
A
S

plane of incidence. The light was incident on the sample with an angle of incidence of about 70°. The reflected beam was passed through a rotatable analyzer and the transmitted intensity observed on a white card.

Certain azimuth settings of the polarizer for the arrangement described above cause the light reflected from the sample to become completely linearly polarized. When the polarizer is at one of these azimuth settings, the analyzer can be rotated to a position where almost no light is transmitted through it. From these angular settings P and A of the polarizer and analyzer, two ellipsometric parameters δ and ψ can be derived as follows.

$$\delta = 270 - 2P$$

$$\psi = A$$

These two parameters are related to the optical constants of GaAs and Si_3N_4 and to the Si_3N_4 cap thickness through the following equation.

$$\tan\psi\, e^{i\delta} = \frac{(r_{01p} + r_{12p}e^{-i2\beta})(1 + r_{01s}r_{12s}e^{-i2\beta})}{(1 + r_{01p}r_{12p}e^{-i2\beta})(r_{01s} + r_{12s}e^{-i2\beta})} \quad \ldots(1)$$

where

$\beta = 2\,(d/\lambda)(n_1^2 - n_0^2\sin^2\phi)^{1/2}$

λ = wavelength of light

d = cap thickness

ϕ_0 = angle of incidence

n_0 = refractive index of air

n_1 = refractive index of cap

r_{01p}, r_{12p}, r_{01s}, r_{12s} are the Fresnel coefficients for p- and s-polarizations for the air-Si_3N_4 and Si_3N_4-GaAs interfaces and are given in Appendix A. Since all optical constants that appear in the above equation are known at room temperature, the only unknown quantity d can be determined once P and A are measured. Both the real and imaginary parts of tan e and the corresponding parts of the right side of Eq(1) should match for the appropriate value of d.

A computer program was written to compute the expression on the right side of Eq (1). The experimental data and calculated results will be included in Chapter 3.

CHAPTER 3

ANALYSIS OF DATA: DETERMINATION OF TEMPERATURE-DEPENDENT REFRACTIVE INDICES OF GaAs AND Si_3N_4

Sample Characteristics

Three samples as described below were used for the time-resolved reflectivity studies:

1) Cr doped GaAs with bare surface (from Crystal Specialties Inc.)

2) 140 Kev Si implanted GaAs; implantation fluence = 2×10^{13} /cm^2 (from Wright Patterson Air Force Base, Ohio). This sample had a 63 nm cap and appeared purple in daylight.

3) 320 Kev Se implanted GaAs; implantation fluence = 2.2×10^{12} /cm^2 (from Honeywell). This sample was also capped and appeared blue in daylight. The cap thickness was determined using null ellipsometry as described below.

Results from Null Ellipsometry

The experimental set-up and the theory for measurement of cap thickness using null-ellipsometry has been briefly discussed in Chapter 2.

wavelength of light = 633 nm (He-Ne laser)

refractive index of cap[18] = 2.02

refractive index of GaAs substrate[19] = $3.86 + i0.198$

angle of incidence = 69.0°

Angles P and A were determined experimentally and had the following values:

$P = -61.3^{\circ}$ and $A = 37.2^{\circ}$

The corresponding values of and are:

$\delta = 32.6^{\circ}$, $\psi = 37.2^{\circ}$

and $\tan \psi e^{i\delta} = 0.64 + 0.41\ i$

The expression on the right-hand side of Eq (1) Chapter 2 was computed for a wide range of cap thicknesses. The values only in a small range centred around the thicknesses which gave the best matching results have been reproduced in Table 1. According to the table, the cap thickness of the sample is estimated to be 79 $\pm$ 1 nm.

Effect of dopants on optical properties of GaAs

Assuming a Gaussian profile in depth for the implanted species it can be shown that the peak concentration for the implanted atoms is given by the expression

$$N_{max} = F/\sigma\sqrt{\pi} \qquad \ldots.(2)$$

where F is the implantation fluence and σ the projected standard deviation. The stopping power of Si_3N_4 is about the same as that of GaAs, and the values of for the second and third samples mentioned above are estimated to be atleast 0.01 um. The peak concentration is estimated to be less than $10^{19}/cm^3$ for all of the above samples. The absorption edge for GaAs is at 1.42 ev, and the photon energy of the probe beam used was 2.41 ev (λ = 514.5 nm) which is well above the edge. Because of the fact that the concentration of the dopants is only a small fraction of the concentration of Ga

TABLE 1 Reflection Ellipsometry: Matching of real and imaginary parts of Equation (1) to determine the thickness of cap for Sample # 3.

Left Hand Side (obtained experimentally) = 0.64 + 0.41 i

Cap thickness (nm)	Right Hand Side (computed) Real part	Imaginary part
68.0	0.364	0.481
68.6	0.376	0.481
69.2	0.389	0.481
69.7	0.401	0.481
70.3	0.413	0.480
70.8	0.427	0.480
71.4	0.440	0.479
72.0	0.454	0.477
72.5	0.469	0.475
73.1	0.483	0.473
73.7	0.498	0.470
74.2	0.513	0.467
77.6	0.611	0.434
78.2	0.628	0.426
78.7	0.645	0.417
79.3	0.663	0.407
79.8	0.680	0.396
80.4	0.697	0.384
81.0	0.715	0.371
81.5	0.732	0.357
82.0	0.748	0.341
82.6	0.765	0.325
83.2	0.780	0.307
83.8	0.795	0.289
84.3	0.810	0.269
84.9	0.824	0.248
85.5	0.836	0.226

According to the above table the cap thickness is estimated to be 78 nm $\sim$ 80nm.

Figure 7 Effect of dopants on absorption coefficient of GaAs (obtained from Ref #20).

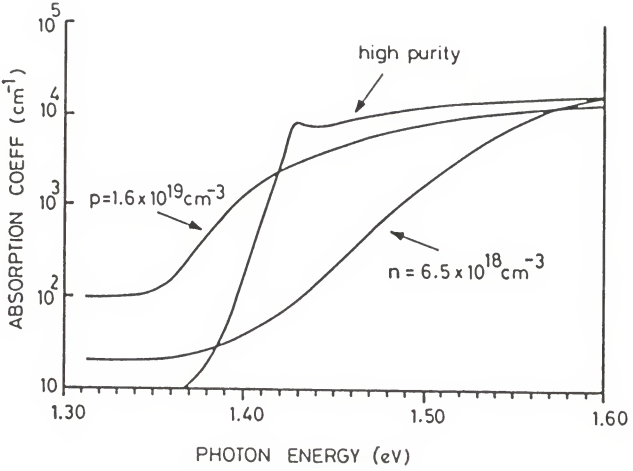
high purity
p=1.6 x 10^19 cm^-3
n = 6.5 x 10^18 cm^-3
ABSORPTION COEFF (cm^-1)
10^5
10^4
10^3
10^2
10
1.30
1.40
1.50
1.60
PHOTON ENERGY (eV)

or As atoms and that the optical constants of GaAs do not depend, at least at room temperature, on the type of doping for photon energies larger than 1.6 ev (see Fig 7), the reflectivity of the samples is not expected to have any dependence on the implanted species.

Features of time-resolved reflectivity traces of capless samples

Fig 8a shows a typical trace of the reflected probe beam intensity during laser irradiation for a bare sample. For annealing energy densities beyond a certain threshold value E_t, the reflectivity R rises from R_0, in time τ_r to R_m, where it is maintained for a time τ_m, before it falls back toward R with a 1/e fall time of τ_f. For a higher value of pulse energy density, the value of R_m is the same, although the duration of high reflectivity is longer (see Fig 8b). It is also worth noting that the trace of the reflected beam intensity for pulse energy densities lower than E_t is significantly different (see Fig 8c) from those obtained with energy densities higher than E_t. For the bare sample the energy density for the onset of melting was found to be 0.05 J/cm^2 and the value of E_t was found to be 0.15 J/cm^2.

It is generally agreed upon that the characteristic rise in reflectivity for $E > E_t$ is because the melt front in the substrate sweeps past the probe depth of the probe beam

Figure 8 Features of Reflectivity vs Time trace for capless samples during pulsed excimer laser irradiation: The traces were recorded with p-polarized probe beam and and angle of incidence=30°
(a) annealing energy density=0.27 J/cm^2, ζ_m=molten phase duration, ζ_f=fall time, R_m=reflectivity during molten phase.
(b) annealing energy density= 0.34 J/cm^2, the melt duration is longer at higher pulse energy density but the reflectivity R_m during the molten phase is the same.
(c) annealing energy density=0.05 J/cm^2, the reflectivity trace is significantly different for pulse energy density lower than the threshold for melting.

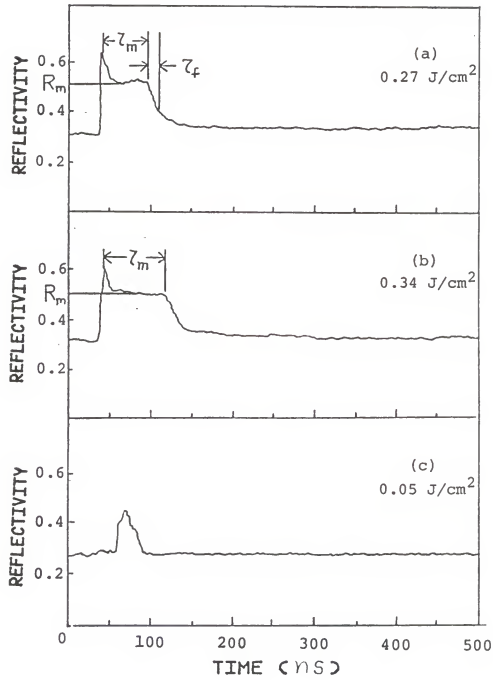
REFLECTIVITY
0.6
R_m
0.4
0.2
τ_m
τ_f
(a)
0.27 J/cm^2
(b)
0.34 J/cm^2
(c)
0.05 J/cm^2
0
100
200
300
400
500
TIME (ns)

within a few nanoseconds after the pulse energy is deposited in the sample. The probe depth in GaAS at room tmperature for light of wavelength 514.5 nm is 54 nm and it is expected to be much less for GaAs in the molten state. In fact, from our data, which will be discussed later in this chapter, we deduce that that the absorption coefficient (α) for GaAs in the molten state is 3.7×10^5 and the corresponding probe depth ($1/2\alpha$) is 14 nm. The fall in reflectivity is similarly explained by the fact that the melt front sweeps back to the surface of the sample as the heat is conducted deeper into the substrate. The value R_m is thus characteristic of molten GaAs and the reflectivity trace is quite different for E < Et because the value of the optical constants of GaAs undergo a discontinuous change during the transition from solid phase to liquid phase. The spikes in Figures 8a and 8b appear to be due to emission from the GaAs substrate.

Reflectivity of capped samples

For the capped samples, equally abrupt changes in reflectivity for the probe beam were expected for energy densities beyond a certain threshold value. In addition the situation is different because the reflectivity in the presence of a cap depends not only on the temperature-dependent optical properties of GaAs but also on the refractive index and cap thickness of the Si_3N_4 layer and the polarization of light. In fact, very different traces were

Figure 9 Reflectivity vs Time for capped samples: These traces were recorded while annealing with the excimer laser.
(a) cap thickness=79 nm; annealing energy density=0.27 J/cm^2; probe beam: s-polarized.
(b) cap thickness=63 nm; annealing energy density=0.27 J/cm^2; probe beam: s-polarized.
(c) cap thickness=59 nm; the Si_3N_4 cap was damaged when energy densities exceeding 0.3 J/cm^2 were used; probe beam: p-polarized.

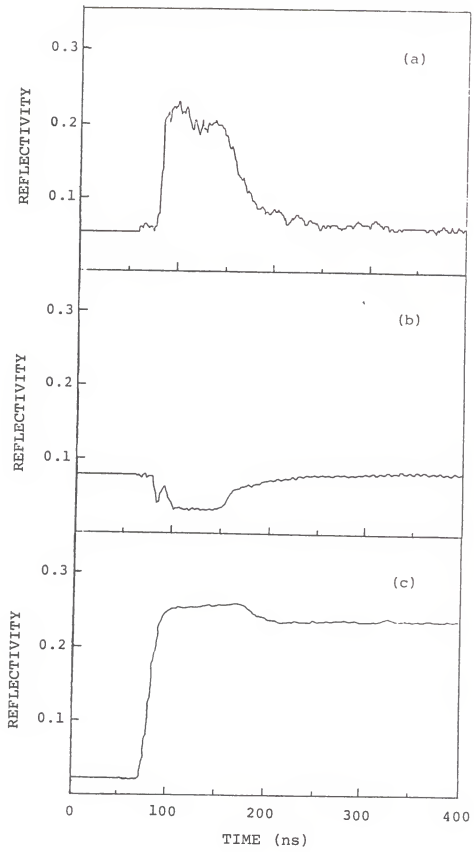
(a)
(b)
(c)
REFLECTIVITY
REFLECTIVITY
REFLECTIVITY
0.3
0.2
0.1
0.3
0.2
0.1
0.3
0.2
0.1
0
100
200
300
400
TIME (ns)

observed with s-polarization when the purple and blue capped samples were annealed with the same energy density of 0.27 J/cm^2 (see Fig 9a & 9b). The rapid changes in reflectivity that take place with in the first 10 ns immediately after the pulse energy is deposited in the sample appear to be the result of rapid changes in the refractive indices of GaAs and Si_3N_4 and an interference effect because of the encapsulating layer. The threshold for the onset of melting was about 0.08 J/cm^2 for both the samples and with annealing energy densities exceeding 0.3 J/cm^2 the caps were damaged resulting in traces similar to the one shown in Fig 9c.

Multiple beam interference

Besides serving the primary purpose of preventing loss of As during annealing, the encapsulating layer of Si_3N_4 also sets up an interference pattern for any radiation that is incident on the sample. A simple model of multiple beam interference with a single transparent layer on a homogeneous substrate was considered to explain the observed traces. In fact, the same model was earlier assumed in deriving the equations for ellipsometric measurement of cap thickness for the samples at room temperature. Two factors that can possibly change the reflectivity of the sample during laser irradiation are: 1) expansion of cap due to heating and 2) change in the temperature-dependent optical constants of Si_3N_4 and GaAs.

Figure 10 Multiple Beam Interference: A model consisting of a thin transparent layer on a substrate can explain the reflectivity of Si_3N_4 capped GaAs samples.

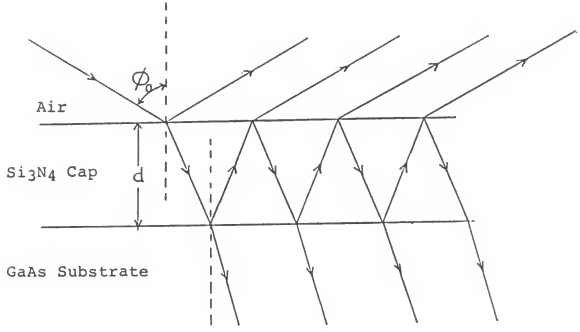
ϕ_0
Air
Si_3N_4 Cap
d
GaAs Substrate

Figure 11 Polarization dependence of Reflectivity: All four traces were recorded during pulsed excimer laser irradiation of a sample having a 63 nm cap.

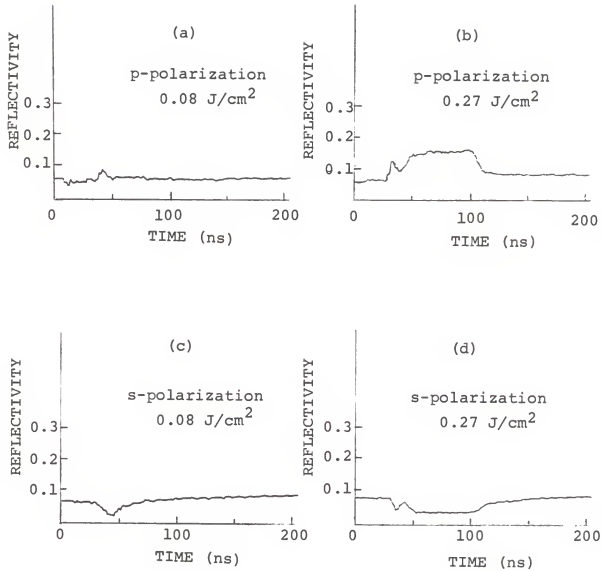
(a)
p-polarization
0.08 J/cm2
REFLECTIVITY
0.3
0.2
0.1
0
100
200
TIME (ns)
(b)
p-polarization
0.27 J/cm2
REFLECTIVITY
0.3
0.2
0.1
0
100
200
TIME (ns)
(c)
s-polarization
0.08 J/cm2
REFLECTIVITY
0.3
0.2
0.1
0
100
200
TIME (ns)
(d)
s-polarization
0.27 J/cm2
REFLECTIVITY
0.3
0.2
0.1
0
100
200
TIME (ns)

reflectivity of the samples on the refractive index of GaAs is through the Fresnel coefficients (see Appendix A).

Determination of Refractive indices of GaAs and Si_3N_4

The experiment was performed with both p- and s polarization for the probe in order to obtain more information without changing the angle of incidence. Fig 11 shows four traces that were recorded while annealing the 63 nm cap sample with the excimer laser. A computer program was written to calculate the values of R_p and R_s, the reflectivities for p- and s-polarizations for a range of cap thickness from 0 nm to 100 nm. The listing of the program is included in Appendix B. The room temperature values of the optical constants for Si_3N_4 and GaAs at λ = 514.5 nm are known.[18, 19] With these known values and a value of 56.0° for angle of incidence the reflectivity of the samples at room temperature could be calculated. A search was then made to determine the optical constants of GaAs and Si_3N_4 at higher temperatures that were consistent with the changes in reflectivities of the probe beam observed for all three samples with p- as well as s-polarization during pulsed laser irradiation. The optical constants that gave the best results are presented in the following table.

Temperature	Refractive index of GaAs		Refractive index of Si_3N_4
	real part	imaginary part	(real)
300°K	4.22	0.38	2.04
1500°K (GaAs solid)	4.9 ± 0.1	0.6 ± 0.1	2.10 ± 0.02
1500°K (GaAs molten)	5.7 ± 0.1	3.0 ± 0.2	2.29 ± 0.02

Table 2

The computed reflectivity as a function of cap thickness with the optical constants stated in the above table have been plotted (see Fig 12).The calculated reflectivities for bare GaAs and the capped samples with cap thicknesses of 63 nm and 79 nm have been marked on the plot. The observed and calculated ratios R_{obs} and R_{calc} for the change in reflectivity during laser irradiation have been placed side by side in Tables 3 & 4. Table 3 contains the values for the case in which the GaAs substrate is just below the melting point of GaAs. Points A through F corresponding to the instants after which the traces gradually return to the room temperature values have been marked on the plots of Fig 13 and are identified with this case. Table 4 is for the case in which the substrate is in the molten state. The uncertainities in these ratios due to possible errors in the measurement of reflected beam intensity have also been

Figure 12 Reflectivity vs Cap thickness for the probe beam: angle of incidence=56.0°; wavelength of pobe beam=514.5 nm; the values of the refractive indices used are as listed in Table 2; cap thicknesses of 63 nm and 79 nm have been marked on the horizontal axes.

(a) p-polarization

(b) s-polarization

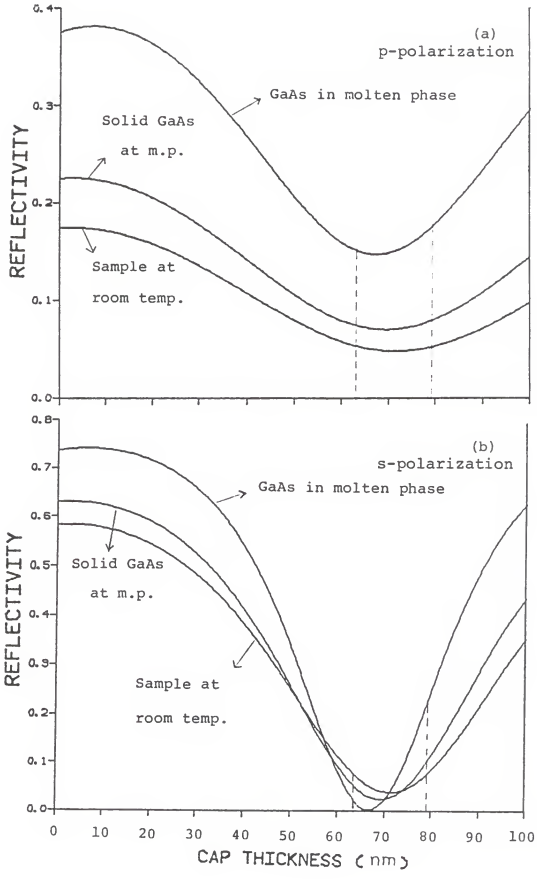
(a)
p-polarization
GaAs in molten phase
Solid GaAs
at m.p.
Sample at
room temp.
REFLECTIVITY
0.4
0.3
0.2
0.1
0.0
(b)
s-polarization
GaAs in molten phase
Solid GaAs
at m.p.
Sample at
room temp.
REFLECTIVITY
0.8
0.7
0.6
0.5
0.4
0.3
0.2
0.1
0.0
0
10
20
30
40
50
60
70
80
90
100
CAP THICKNESS (nm)

Figure 13 Reflectivity traces used to determine refractive indices of GaAs and Si_3N_4: (a) and (b): capless sample annealed at 0.22 J/cm^2 (c) and (d): cap thickness=63 nm ,energy density=0.27 J/cm^2, (e) and (f): cap thickness=79 nm, energy density=0.27 J/cm^2

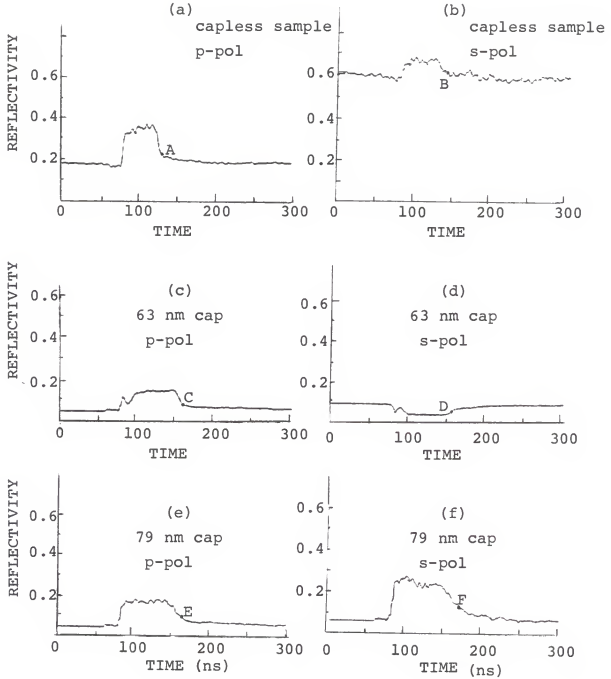
(a)
capless sample
p-pol
(b)
capless sample
s-pol
(c)
63 nm cap
p-pol
(d)
63 nm cap
s-pol
(e)
79 nm cap
p-pol
(f)
79 nm cap
s-pol
REFLECTIVITY
0.6
0.4
0.2
A
B
C
D
E
F
0
100
200
300
TIME
TIME (ns)

TABLE 3: Ratio of change in reflectivity of the samples when the GaAs substrate is in solid phase but at the melting point.

For p-polarization		
cap thickness	Observed factor	Calculated factor
0 nm	1.35 ± 0.10	1.30
63 nm	1.28 ± 0.15	1.39
79 nm	1.7 ± 0.2	1.52
For s-polarization		
cap thickness		
0 nm	1.10 ± 0.06	1.08
63 nm	0.75 ± 0.06	0.7
79 nm	1.35 ± 0.15	1.35

TABLE 4: Ratio of change in reflectivity of the samples when the GaAs substrate is in the molten phase.

For p-polarization		
cap thickness	Observed factor	Calculated factor
0 nm	2.11 ± 0.15	2.16
63 nm	2.9 ± 0.3	2.83
79 nm	3.5 ± 0.3	3.31
For s-polarization		
cap thickness		
0 nm	1.17 ± 0.08	1.26
63 nm	0.37 ± 0.04	0.34
79 nm	3.2 ± 0.2	2.97

indicated in the table. The optical constants for GaAs and Si_3N_4 given in Table 2 were arrived at my minimizing first through a grid search and then through a more refined gradient search the sum of squares of

$$\frac{R_{calc} - R_{obs}}{R_{obs}}$$

This sum is comprised of six terms corresponding to p- and s-polarization and the three different samples. The uncertainities in the values of the optical constants were determined on the basis of the uncertainities in the ratios R_{obs} of Tables 3 & 4.

Reflectivity traces similar to the ones discussed above were obtained also using ~10 ns dye laser pulses for annealing (λ = 728 nm). The dye laser used was Lambda Physik Model FL2002 and it was optically pumped with a Nd: YAG laser (Quanta-Ray). The angle of incidence for the argon ion probe beam was 30°. Fig 14 shows some traces that were obtained for p-polarization with a sample that had a 60 nm cap. The optical constants in Table 2 explain these traces equally well.

Figure 14 Reflectivity vs Time during dye laser annealing: cap thickness=59 nm, probe beam was p-polarized and incident at 30°.

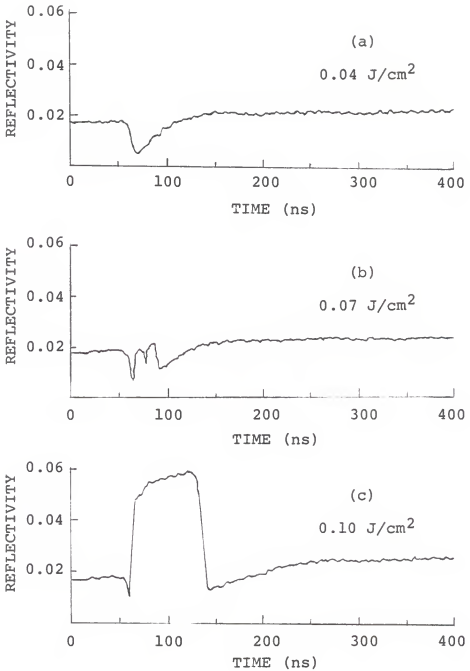
REFLECTIVITY
0.06
0.04
0.02
(a)
0.04 J/cm2
0
100
200
300
400
TIME (ns)
REFLECTIVITY
0.06
0.04
0.02
(b)
0.07 J/cm2
0
100
200
300
400
TIME (ns)
REFLECTIVITY
0.06
0.04
0.02
(c)
0.10 J/cm2
0
100
200
300
400
TIME (ns)

CHAPTER 4

CONCLUSION

Time-resolved reflectivity measurements made to date have been mostly used to construct mathematical models to describe the process of melting and rapid solidification that occurs in pulsed laser processing of GaAs and other semiconductors.[20,21] Several parameters such as pulse energy density, thermal conductivity, heat capacity, absorption coefficient, reflectivity, latent heat of melting, diffusivities for the implanted ions etc. are used as inputs to the mathematical model to simulate reflectivity traces of a probe beam during irradiation. A good model should be able to explain a reflectivity trace well, just as it should make accurate predictions for results from other studies such as RBS, TEM, etc.. The characteristics of reflectivity data most often sought to be understood include the threshold energy density for melting, and features of reflectivity traces such as the melt duration and shapes of the rising and falling edges. Time-resolved reflectivity measurements have been conducted also to detemine the optical properties of silicon during excimer laser irradiation.[24]

In the experiment discussed in this thesis the focus was on determining the optical constants of molten GaAs and GaAs just below the melting point at a wavelength of 514.5 nm. The value of the refractive index suggested in Table 2

of Chapter 3 for molten GaAs is (5.7 ± 0.2) + i (3.0 ± 0.2). The corresponding value of the absorption coefficient given by

$$\alpha = 2\pi \, \mathrm{Imag}(n) \, / \, \lambda$$

is about 3.7 x 10^5/cm. For GaAs just below the melting point the refractive index suggested is (4.9 ± 0.1) + i (0.6 ± 0.1) (see Table 2). Both the real and imaginary parts of the refractive index are larger than the corresponding room temperatue values of 4.22 and 0.38. This observation is consistent with what one might expect to happen if the E_1 gap of GaAs which is 2.91 ev at room temperature drops to a value that lies closer to the probe beam energy of 2.42 ev when the sample is heated.

Similar experiments can be performed with probe beams of different wavelengths to determine the temperature dependent optical properties of GaAs at other frequencies.

The melt duration and the threshold energy density for melting and for damage to the cap were found to vary slightly from sample to sample. Their values were markedly different for the two different wavelengths used for annealing: 308 nm from the excimer laser and 728 nm from the dye laser. The threshold for damage to the cap was about 0.3 J/cm^2 with the excimer laser and only about 0.1 J/cm^2 with the dye laser. It is very likely that the difference is again due to an interference pattern that is set up when the sample is irradiated. Depending on the cap thickness and the

wavelength of the annealing pulse the effective energy that the substrate receives is possibly quite different from case to case even for the same value of incident pulse energy. In a case such as this one in which we wish to calculate the energy transmitted through the cap while the temperature of the substrate is changing rapidly, it will be inappropriate to use the simple model that has been used to calculate the reflectivity of the probe beam. But the problem can be solved with a more realistic model which takes in to consideration the rapid changes in the temperature of the sample, and knowledge of the optical constants as a function of temperature will be useful here.

Obviously, more work needs to be done to understand the melting and rapid solidification, and the resulting crystal defects that are associated with pulsed laser annealing of GaAs. It is hoped that with a better understanding of the phenomenon it would be possible to create conditions under which better activation and higher mobilities are obtained.

APPENDIX A

Fresnel coefficients for p- and s-polarization

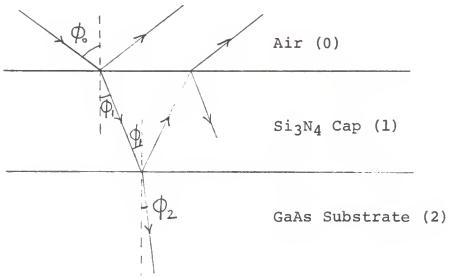

$$r_{01p} = \frac{N_1 \cos_0 - N_0 \cos_1}{N_1 \cos_0 + N_0 \cos_1}$$

$$r_{12p} = \frac{N_2 \cos_1 - N_1 \cos_2}{N_2 \cos_1 + N_1 \cos_2}$$

$$r_{01s} = \frac{N_0 \cos_0 - N_1 \cos_1}{N_0 \cos_0 + N_1 \cos_1}$$

$$r_{12s} = \frac{N_1 \cos_1 - N_2 \cos_2}{N_1 \cos_1 + N_2 \cos_2}$$

N_0 = refractive index of air

N_1 = refractive index of Si_3N_4 cap

N_2 = refractive index of GaAs (complex number)

APPENDIX B

Listing of program to calculate Reflectivity (p-polarization)

```
c       REF P.for (FOR P (PARALLEL POLARIZATION THROUGH NON-ABSORBING CAP
        dimension REF(201)
        complex nc,b12,c12,d12,e12,R12,cph,p1,p2,RA
        type 10

c       The next section is to accept input data.
10        format(' type angle of incidence in degrees ')
          accept*,theta0
          theta0 = (theta0/57.295799)
          type 12
12        format (' type wavelength of light in angstroms.')
          accept*,wave
          type 15
15        format(' type  refractive index of cap ')
          accept 18,cap
18        format(2f8.5)
          type 19,cap
19        format(' ref. index of cap accepted as', 2f7.3)
          type 20
20        format(' type refractive index of substrate (both parts)')
          accept 30,nc
30        format (2f8.5)
          type 35,nc
35        format(' nc accepted as ',2f7.3)

c       This section is to compute the Fresnel coefficient R01.
          b01 = cap*cos(theta0)
          a = (sin(theta0))*sin(theta0)
          c01 = 1/(cap*cap)
          d01 = a*c01
          e01 = sqrt(1-d01)
          R01 = (b01-e01)/(b01+e01)

c       This section is to compute the Fresnel coefficient R12
          stheta1 = (sin(theta0))/cap
          theta1 = asin(stheta1)
          b12 = nc*cos(theta1)
          c12 = 1/(nc*nc)
          d12 = a*c12
          e12 = cap*sqrt(1 - d12)
          R12 = (b12-e12)/(b12+e12)

c       This section is to print-out the input parameters.
          theta0 = (theta0)*57.295799
          print 40,theta0
40        format(' angle of incidence = ',f4.1)
```

```
        print 50,wave
50      format(' wavelength of light in A (P polarization)=    ',f6.1)
        print 60,cap
60      format(' ref.index of cap used= ', f8.5)
        print 70,nc
70      format('real and imag parts of ref. index of substrate ',2f8.5)
        print 80

c     This section is to comute the reflectivity of the sample as
c     a function of cap thickness.
80      format('  Cap thickness (A)     Reflectivity')
        thic = 0
      do 100 i = 1,201



        ratio = thic/wave
        ph = -4*3.1415927*cap*cos(theta1)*ratio
        x = cos(ph)
        y = sin(ph)
        cph = x + (0.0,1.0)*y
        p1 = R01 + R12*cph
        p2 = 1 + R01*r12*cph
        RA = p1/p2
        RAR = real(RA)
        RAI = aimag(RA)
        REF(i) = RAR*RAR + RAI*RAI
        print 90,thic,REF(i)
90      format('    ',f5.1,'              ',f10.5)
        thic = thic + 5.0
100   continue
      stop
      end
```

Listing of program to calculate Reflectivity (s-polarization)

```
c       REF S.for (FOR S (PERPENDICULAR) POLARIZATION THROUGH NON-ABSORBING CA
        dimension REF(201)
        complex  nc,c12,d12,e12,R12,cph, p1,p2,RA

c       This section is to accept input parameters.
          type 10
10        format(' type angle of incidence in degrees ')
          accept*,theta0
          theta0 = (theta0/57.295799)
          type 12
12        format (' type wavelength of light in angstroms.')
          accept*,wave
          type 15
15        format(' type  refractive index of cap ')
          accept 18,cap
18        format(2f8.5)
          type 19,cap
19        format(' ref. index of cap accepted as', 2f7.3)
          type 20
20        format(' type refractive index of substrate (both parts)')
          accept 30,nc
30        format (2f8.5)
          type 35,nc
35        format(' nc accepted as ',2f7.3)

c       This section computes the Fresnel coefficient R01
          b01 = cos(theta0)
          a = (sin(theta0))*sin(theta0)
          c01 = 1/(cap*cap)
          d01 = a*c01
          e01 = cap*sqrt(1-d01)
          R01 = (b01-e01)/(b01+e01)

c       This section is to compute the Fresnel coefficient R12
          stheta1 = (sin(theta0))/cap
          theta1 = asin(stheta1)
          b12 = cap*cos(theta1)
          c12 = 1/(nc*nc)
          d12 = a*c12
          e12 = nc*sqrt(1 - d12)
          R12 = (b12-e12)/(b12+e12)

c       This section is to print the input parameters on the print-out.

          theta0 = (theta0)*57.295799
          print 40,theta0
40        format(' angle of incidence = ',f4.1)
```

```
      print 50,wave
50    format(' wavelength of light in A (s-polarization)=    ',f6.1)
      print 60,cap
60    format(' ref.index of cap used= ',2f8.5)
      print 70,nc
70    format('real and imag parts of ref. index of substrate ',2f8.5)
      print 80

c     This section computes the reflectivity of the sample as a function
c     cap thickness.
80    format('  Cap thickness (A)    Reflectivity')
      thic = 0




      do 100 i=1,201
        ratio = thic/wave
        ph = -4*3.1415927*cap*cos(theta1)*ratio
        x = cos(ph)
        y = sin(ph)
        cph = x + (0.0,1.0)*y
        p1 = R01 + R12*cph
        p2 = 1 + R01*R12*cph
        RA = p1/p2
        RAR = real(RA)
        RAI = aimag(RA)
        REF(i) = RAR*RAR + RAI*RAI
        print 90,thic,REF(i)
90      format('     ',f6.1,'              ',f10.5)
        thic = thic + 5.0
100   continue
      stop
      end
```

Listing of program used to operate the Tektronix 7912AD Digitize:

```
1000 REM ********************************************************************
1010 REM *      FILE:  ACQ.BAS
1020 REM ********************************************************************
1030 REM <<<<<<<<<<<<<<<<<<<<<<<<<<INITIALIZATION>>>>>>>>>>>>>>>>>>>>>>>>>>>>
1040 PRINT CHR$(27);"[?0L"\PRINT\PEM - CLEAR SCREEN\UNSCHEDULE ALL
1050 PRINT "DATA ACQUISITION PROGRAM FOR TEKTRONIX 7912AD"
1060 PRINT "VERSION 4.14.87"\PRINT
1070 PRINT "THIS PROGRAM ACQUIRES NX64 WAVEFORMS FROM 7912AD"
1080 PRINT "DISPLAYS THE AVERAGE OF THESE WAVEFORMS AND GIVES"
1090 PRINT "THE USER AN OPTION TO STORE THE AVERAGE WAVEFORM ON DISK"
1100 PRINT
1110 PRINT "IF YOU WANT OT KEEP THE CURRENT DIGITIZER SETTINGS, MAKE SURE
1120 PRINT "THE OPERATING MODE IS TV, LOCAL."\PRINT
1130 PRINT "PRESS A KEY TO PROCEED"
1140 WAIT 1000\WAIT
1150 PRINT
1160 PRINT "INITIALIZING DEVICES:"
1170 PRINT "     LOADING CLOCK DRIVER"\LOAD "CLK.SPS"
1180 PRINT "     LOADING IEEE 488 DRIVER"\LOAD "GPI.SPS"
1190 PRINT "     ASSIGNING INTERFACE ADDRESSES"\LA=32\TA=64\SA=96
1200 PRINT "     CLEARING INTERFACE LINES"\SIFLIN @0,"IFC"\WAIT 500
1210 PRINT "     CLEARING DIGITIZER"\SIFCOM @0,"DCL"\WAIT 500
1220 PRINT "     ENABLING SERIAL POLL"\SIFCOM @0,"SPE"\WAIT 500
1230 PRINT "     SETTING TIMEOUT VALUE TO 30000 MS"\SIFTO @0,30000\WAIT 50
1240 PRINT
1500 REM <<<<<<<<<<<<<<<<<<<<<<TARGET DEFECTS CORRECTION>>>>>>>>>>>>>>>>>>>>
1510 PRINT\REM  THIS SECTION DIGITIZES CRT TARGET DEFECTS AND LOADS DEFECT
1520 REM        IN THE DIGITIZER'S DEFECTS ARRAY
1530 PRINT "WILL SCAN FOR TARGET DEFECTS.  TURN OFF INTENSITY KNOBS."
1540 PRINT\PRINT "PRESS A KEY TO PROCEED."
1550 PRINT
1560 WAIT 500\WAIT
1570 INPREQ CHAR,NOECHO GOSUB 4010
1580 PRINT "SWITCHING TO DIGITAL MODE"\PUT "MODE DIG" INTO @0,LA,SA\WAIT 5
1590 PRINT "ENABLING SRQ ON OPC"\PUT "OPC ON" INTO @0,LA,SA\WAIT 5000
1600 PRINT "DIGITIZING DEFECTS 64 TIMES"\PUT "DIG DEF,64" INTO @0,LA,SA
1610 PRINT
1620 REM     IF UNABLE TO DETECT SRQ AFTER 30 SECONDS ASSUME DIG DEF COMPLE
1630 REM
1640 SCHEDULE AFTER 30 GOSUB 1710
1650 REM
1660 REM     POLL DIGITIZER FOR SRQ WHICH INDICATES COMPLETION OF DIG DEF
1670 REM     IF SRQ IS DETECTED STOP AND LOAD DEFECTS INTO DEFECTS ARRAY
1680 REM
1690 WAIT 100\POLL @0,SB,PA,SS,TA,SA\IF SB<>66 THEN 1690
1700 UNSCHEDULE GOSUB 1710
1710 PUT "DEF LOAD" INTO @0,LA,SA
1720 INPREQ
2000 REM <<<<<<<<<<<<<<<<<<<<<<<<SIGNAL AVERAGING>>>>>>>>>>>>>>>>>>>>>>>>>>
2010 ONERR NOWARN
2020 N=1\R=1
2090 PRINT "SET THE DIGITIZER TO ACQUIRE DATA AS SOON AS IT GOES TO"
2100 PRINT "TO LOCAL, TV MODE."\PRINT
2110 PRINT "PRESS A KEY TO PROCEED."
2120 PUT "MODE TV" INTO @0,LA,SA
2130 SIFCOM @0,LA,SA,"GTL"\WAIT 500
2140 WAIT
```

```
2150 PRINT\PUT "HS1?" INTO @0,LA,SA
2160 GET A$ FROM @0,TA,SA
2170 HS=VAL(SEG(A$,5,LEN(A$)-1))\HS=HS/51.2\VS=1\HP$="S"\VP$=" "
2180 REM
2190 PRINT " SWITCHING TO DIGITAL MODE"\PUT "MODE DIG" INTO @0,LA,SA\WAIT 50
2200 PRINT " ENABLING SERIAL POLL"\SIFCOM @0,"SPE"\WAIT 500
2210 PRINT " ENABLING SP0 ON OPC"\PUT "OPC ON" INTO @0,LA,SA\WAIT 1000
2220 INTEGER A(511)
2240 ONERR EX GOTO 2500
2270 PUT "DIG SA,1" INTO @0,LA,SA
2300 POLL @0,SB,PA,SS,TA,SA
2310 IF SB<>66 THEN 2300
2330 PUT "READ SA" INTO @0,LA,SA
2340 IFDTM @0,"PAK","HBF"
2350 READBINARY A FROM @0,TA,SA\P=A
2580 REM
2590 WAVEFORM WP IS P,HS,HP$,VP$
2600 PAGE\GRAPH WP
2620 PRINT CHR(27)$"2"\PRINT CHR(7)$"PRESS A KEY TO PROCEED."
2630 WAIT 1000\WAIT
2640 PAGE\INIT6\PAGE\PPRINT CHR(27)$"2"
3000 REM <<<<<<<<<<<<<<<<<<<<RECORD KEEPING SECTION>>>>>>>>>>>>>>>>>>>>>>>>>>>
3010 REM
3020 PRINT
3030 PRINT\PRINT "DO YOU WANT TO LOG THIS EXPERIMENT (Y/N)"$\INPUT AA$
3040 IF AA$<>"Y" THEN 3220
3050 PRINT
3060 PRINT "MAKE SURE YOU HAVE A FORMATTED DS/DD DISKETTE IN THE DISK"
3070 PRINT "DRIVE.  PRESS A KEY TO PROCEED."
3080 WAIT 500\WAIT
3090 PRINT
3100 PRINT "DESCRIPTION OF EXPERIMENT:"
3110 INPUT A$\INPUT AC$
3120 PRINT "DATA FILENAME (SPECIFY FILENM.EXT)"$\INPUT AF$
3130 PRINT "DATA DISKETTE VOLUME ID"$\INPUT VN$
3140 ONERR NOWARN\PRINT "WHICH SIDE (0 OR 1)"$\INPUT SD\IF SD<>1 THEN SD=0
3150 LOAD "DY"\ONERR EX GOTO 3680
3160 IF SD=0 THEN OPEN #1 AS DY0:AF$ FOR WRITE
3170 IF SD=1 THEN OPEN #1 AS DY1:AF$ FOR WRITE
3180 DATE D$
3190 WRITEU #1,N*64,VS,HS,P
3200 WRITE #1:A$,AC$,D$,VN$
3210 CLOSE #1\DELETE P
3220 PRINT "DO YOU WANT TO DO MORE SCANS(Y/N)";
3230 INPUT AA$
3240 IF AA$="Y" THEN 2000
3250 SIFCOM @0,LA,SA,"GTL"
3260 OLD "CHOICE.BAS"
3500 REM <<<<<<<<<<<<<<<<<<ERROR AND INTERRUPT HANDLER>>>>>>>>>>>>>>>>>>>>
3510 IF EX(1)<>80 THEN 3620
3520 IF EX(2)<>8 THEN 3530\CLOSE #1\CANCEL "TEMP.DAT"\GOTO 3540
3530 IF EX(2)<>5 THEN 3550\CLOSE #1\CANCEL "TEMP.DAT"
3540 ONERR RETURN GOTO 2250
3550 IF EX(2)<>16 THEN 3560\PPINT "DISK IS FULL."\GOTO 3580
3560 IF EX(2)<>17 THEN 3570\PPINT "DIRECTORY IS FULL."\GOTO 3580
3570 IF EX(2)<>18 THEN 3650\PPINT "FILE SIZE > 1/2 REMAINING SPACE."
3580 PRINT "ABORTING PROCEDURE.  TPY CLEANING UP DL0:, THEN RUN THE "
```

```
3590 PRINT "  PROGRAM AGAIN."\CLOSE #1\CANCEL "TEMP.DAT"
3600 INPREQ
3610 STOP
3620 IF EX(1)<>73 THEN 3630\PRINT "DIGITIZER ERROR..."\GOTO 3640
3630 IF EX(1)<>68 THEN 3850\PRINT "DIGITIZER ERROR..."
3640 INPREQ
3650 PRINT "TURN OFF, THEN ON AGAIN TO RESET."
3660 PRINT "PRESS A KEY TO PROCEED."\WAIT
3670 ONERR RETURN GOTO 1000
3680 IF EX(1)<>80 THEN 3810
3690 IF EX(2)<>8 THEN 3700\CLOSE #1\ONERR RETURN GOTO 3160
3700 IF EX(2)<>5 THEN 3730\PRINT CHR(7);"FILENAME ALREADY EXISTS."
3710 PRINT "ENTER ANOTHER FILENAME"\INPUT AF$
3720 ONERR RETURN GOTO 3160
3730 IF EX(2)<>16 THEN 3740\PRINT "DISK IS FULL."\GOTO 3760
3740 IF EX(2)<>17 THEN 3750\PRINT "DIRECTORY IS FULL."\GOTO 3760
3750 IF EX(2)<>11 THEN 3850\PRINT "FILE SIZE > 1/2 REMAINING SPACE."
3760 CLOSE #1\PRINT "TRY OTHER SIDE (Y/N)";
3770 INPUT D$\IF D$<>"Y" THEN 3790\SD=SD+1\IF SD>1 THEN SD=0
3780 ONERR RETURN GOTO 3160
3790 PRINT "LOAD A NEW DISK THEN PRESS A KEY TO PROCEED."\WAIT
3800 ONERR RETURN GOTO 3160
3810 IF EX(1)<>83 THEN 3850\IF EX(2)<>15 THEN 3850
3820 PRINT CHR(7);AF$;" IS AN ILLEGAL FILE NAME."
3830 PRINT "ENTER ANOTHER FILENAME."\INPUT AF$
3840 ONERR RETURN GOTO 3160
3850 PRINT "THIS IS AN UNEXPECTED ERROR... CHECK TEK MANUALS."
3860 PRINT "ERROR CODE: ";CHR(EX(1));EX(2)
3870 PRINT "AT LINE: ";\LIST EX(0)\INPREQ
3880 PRINT "DO YOU WANT TO RERUN(R),RETURN TO MENU(M) OR QUIT(Q)";
3890 INPUT D$\IF D$<>"R" THEN 3900\CLOSE #1\CANCEL "TEMP.DAT"\OLD "ACQ"
3900 IF D$<>"M" THEN 3910\CLOSE #1\CANCEL "TEMP.DAT"\OLD "CHOICE"
3910 INPREQ
3920 STOP
3930 INPUT A$\IF A$<>CHR(3) THEN 3940\GOTO 2320
3940 IF A$<>CHR(1) THEN 3990\PRINT CHR(7);"ABORTING SCAN..."
3950 CLOSE #1\CANCEL "TEMP.DAT"\INPREQ
3960 PRINT "DO YOU WANT TO RETURN TO MENU (M), DO ANOTHER SCAN (S) OR"
3970 PRINT "RESTART THE PROGRAM (R)";\INPUT D$
3980 IF D$="M" THEN OLD "CHOICE"\IF D$="R" THEN OLD "ACQ"\GOTO 2000
3990 TIME\IF I>=N THEN PRINT "STILL CALCULATING THE AVERAGE WAVEFORM."
4000 IF I<N THEN PRINT "NOW TAKING THE ";I+1;"TH SET OF 64 WAVEFORMS."
4010 RETURN
```

REFERENCES

1. Shtyrkov, E. I., Khaibullin, I. B., Zaripov, M. M., Galjatudinov, M. F., and Bayazitov , R. M. (1976). Sov. Phys.-Semicond. 9, 1309.

2. Williams, J. S., and Austin, M. M. (1980b). Appl. Phys. Lett. 36, 994.

3. Williams, J. S., and Harrison, H. B. (1981). In "Laser and Electron Beam Solid Interactions and Materials Processing" (J.F.Gibbons, L. D. Hess, and T. W. Sigmon, eds.),p.209. North-Holland Publ., New York.

4. Barnes, P. A., Leamy, H. J., Poate, J. M. , Ferris, S. D., Williams, J. S., and Celler, G. K. (1979),In "Laser-Solid interactions and Laser Processing" (S. D. Ferris, H. J. Leamy, and J. M. Poate, eds.), p. 647. Am. Inst. Phys., New York.

5. Lou, C. Y., and Somorjai, G. A. (1971). J. Chem. Phys. 55, 4554.

6. Picraux, S. T., (1973). In "Ion Implantation in Semiconductors and Other Materials" (B. L. Crowder, ed.), p. 641. Plenum Press, New York.

7. Barnes, P. A., Leamy, H. J., Poate, J. M., Ferris, S. D., Williams, J. S., and Celler, G. K. (1978). Appl Phys. Lett. 33, 965.

8. Sealy, B. J., Kular, S. S., Stephens, K. G., Croft, R., and Palmer, A. (1978). Electron. Lett. 14,720.

9. Inada, T., Tokunaga, K., and Taka, S. (1979b). Appl. Phys. Lett. 35, 546.

10. Badawi, M. H., Akintunde, J. A., Sealy, B. J., and Stephens, K. G. (1979). Electron. Lett. 15, 448.

11. Inada, T., Kato, S., Maeda, Y., and Tokunaga, K. (1979a). J. Appl. Phys. 50, 6000.

12. Lowndes, D. H., Cleland, J. W., Fletcher, J., Narayan, J.,Westbrook, R. D., Wood, R. F., Christie, W. H., and Eby, R. E.,(1981b). In "Proceedings of the Fifteenth Photovoltaic Specialists Conference", P. 45. IEEE, New York.

13. Lidow, A., Gibbons, J. F., Deline, V. R., and Evans, C. A.,Jr. (1980). J. Appl.Phys. 51, 4130.

14. Davies, E. D., Ryan, T. G., and Lorenzo, J. P. (1980a). Appl. Phys. Lett. 37, 443.

15. Davies, E. D., Lorenzo, J. P., and Ryan, T. G. (1980b). Appl. Phys. Lett. 37, 612.

16. Davies, E. D., Kennedy, E. F., Ryan, T. G., and Lorenzo, J. P. (1981). In "Laser and Electron Beam Solid Interactions and Materials Processing" (J. F. Gibbons, L. D. Hess, and T. W. Sigmon, eds.), p.247. North-Holland Publ., New York.

17. Popov, W. A., Bulletin EG, Optical Spectra - May, 1977.

18. Handbook of Optical constants, Edited by Edward D. Palik, Naval Research Laboratories, Washington, DC (1985)

19. Aspnes, D. E. and Studna, A. A. Physical Review B 27, N0 2, 15 Jan 1983.

20. Casey, H. C. and Stern, F., J. Appl. Phys, 47, 631 (1976)

21 Handbook of Electronic Materials Volume 6: Silicon Nitride for Microelectronic Applications; Part 2: Applications and Devices, John T. Milek

22. Lowndes, D. H., and Wood, R. F. (1981). Appl. Phys. Lett. 38,971.

23. Auston, D. H., Golovchenko, J. A., Simons, A. L., Slusher, R. E., Smith, P. R., Surko, C. M., and Venkatesan, T. N. C. (1979). Am. Inst. Phys. Conf. Proc. 50, 11.

24. Jellison, G. E., Lowndes, D. H. Mat. Res. Soc. Symp. Proc Vol. 35. 1985 Materials Research Society

TIME-RESOLVED REFLECTIVITY STUDY OF PULSED-LASER-IRRADIATED, Si_3N_4-CAPPED GaAs

by

AJIT BHAT

B.Tech, I.I.T.-Kanpur, 1982, M.Tech, I.I.T.-Delhi, 1984

AN ABSTRACT OF A MASTER'S THESIS

submitted in partial fulfillment of the
requirements for the degree

MASTER OF SCIENCE

Department of Physics

KANSAS STATE UNIVERSITY

Manhattan, Kansas

1987

ABSTRACT

The time-resolved reflectivity of Si_3N_4-capped GaAs has been studied under pulsed laser annealing conditions. Depending on the pulse energy density, the reflectivity of a probe beam incident on the irradiated area is modified for up to two hundred nanoseconds, and the reflectivity during this period is determined by the temperature-dependent optical properties of GaAs and Si_3N_4, the thickness of the encapsulating layer and the wavelength of the probe beam. We have recorded the reflectivity to determine the threshold annealing energy density for melting of GaAs, and have used the interference effect of a thin transparent layer on a substrate to explain the observed reflectivity. We have used the observed reflectivity and this model to arrive at a set of values for the real and imaginary parts of the refractive index at = 514.58 nm of molten GaAs, of solid GaAs just below the melting point and Si_3N_4 at the melting point of GaAs.